

Aspects of Causality in Parallelisable Implicit Evolution Scheme

P. Khavari¹, C. C. Dyer^{1,2}

¹ Department of Astronomy and Astrophysics, University of Toronto, 50 Saint George Street,
Toronto, ON, M5S 3H4, Canada

² Department of Physical and Environmental Sciences, University of Toronto at Scarborough, 1265 Military Trail, Toronto, ON, M1C 1A4, Canada

E-mail: khavari@astro.utoronto.ca

E-mail: dyer@astro.utoronto.ca

Abstract. A (3+1)-evolutionary method in the framework of Regge Calculus, essentially a method of approximating manifolds with rigid simplices, makes an excellent tool to probe the evolution of manifolds with non-trivial topology or devoid of symmetry. The “Parallelisable Implicit Evolution Scheme” is one such method. Causality however, is an aspect of this method that has been barely investigated. In this paper, we show how causality can be accounted for in this evolutionary scheme. The revised algorithm is illustrated by a preliminary application to a skeletonised spherical Friedmann-Lemaître-Robertson-Walker universe.

PACS numbers: 04, 04.25.D, 04.20.Gz

Submitted to: *Class. Quantum Grav.*

1. Introduction

Regge Calculus [1] is a numerical method in general relativity that trades curved manifolds for skeletonised space-times. Considered a finite element method, Regge Calculus approximates a manifold using rigid simplices, higher dimensional generalisation of triangles and tetrahedra. Once an n -dimensional manifold is approximated by n -dimensional simplices, the intrinsic curvature is concentrated on sub-simplices of co-dimension two; the geometry is then flat everywhere within the simplices. The amount of curvature residing on the so-called hinge or bone (sub-simplex of co-dimension two) is then represented by the “deficit angle” associated with the bone [1]. In this formalism, the dynamical variables are the edge lengths of the simplicies which indeed play the role of the metric in the continuum limit.

In addition to being a powerful tool for investigation of problems devoid of symmetry, today Regge Calculus is considered a promising approach in the search for a theory of Quantum Gravity (see the extensive review by Hamber [2]). We believe that Regge Calculus is also an excellent method to incorporate non-trivial topology into

general relativity, which only provides one with local geometry and gives very little information about global features of a manifold including its topology.

One can examine the evolution of a space-time with non-trivial topology using a (3+1)-evolutionary method in the context of Regge Calculus. One such evolutionary scheme, entitled “Parallelisable Implicit Evolution Scheme”, was presented by Barrett et al. [3] based on an earlier work by Sorkin [4]. Causality is an aspect of this algorithm that has not been investigated thoroughly and it has not been incorporated into this algorithm properly. In their seminal paper on “Parallelisable Implicit Evolution Scheme” (PIES), also known as “Sorkin Triangulation”, considering the particular method of triangulation and the causal structure of the skeletonised manifold, Barrett et al. place a restriction on the type of edges that connect two consecutive triangulated spatial hypersurfaces so that causality is not violated. They indicate, however, that causality, in their scheme, is an issue that requires further investigation. As will be described later, the restriction imposed by Barrett et al. indeed prevents the time-like paths of evolving vertices from colliding with their neighbors, but this restriction does not account for causality. PIES, as presented by Barrett et al., does not produce the expected results when implemented to examine the evolution of a skeletonised Friedman-Lemaître-Robertson-Walker spherical universe. In particular, the evolution of this lattice universe stops well before the spatial volume becomes zero. This problem is known as the “stop point” problem. We are confident that the “stop point” problem arises because causality is not accounted for in PIES.

In this paper, we show how causality can be incorporated into PIES properly and what changes must be made so that the Courant condition is satisfied. The inclusion of causality, as done in this paper, resolves the “stop point” problem as will be described in detail in section (3). We believe that by accounting for causality, we have brought the “Parallelisable Implicit Evolution Scheme” a step closer into being a highly efficient tool in examining the evolution of skeletonised manifolds.

Section (2) briefly reviews the “Parallelisable Implicit Evolution Scheme” and describes the problem of causality. Sections (3) and (4) discuss how causality can be included in this evolutionary scheme. In section (5), we illustrate the revised algorithm by applying it to successfully reconstruct a skeletonised spherical Friedmann-Lemaître-Robertson-Walker (FLRW) universe. Section (6) closes this paper with some concluding remarks.

2. A Brief Review of “Parallelisable Implicit Evolution Scheme” Approach

As described in the introduction, Barrett et al. developed a (3+1)-evolutionary method in the context of Regge Calculus [3]. The so-called “Parallelisable Implicit Evolution Scheme”, considers a triangulated spatial section and assumes that all the information pertaining to the triangulation of the space-time up to and including this particular spatial hypersurface is known. It then prescribes how one can evolve this skeletonised spatial hypersurface into the future.

More specifically, this method starts with an arbitrary vertex on the initial hypersurface. It then introduces an evolved counter-part to this vertex in the temporal

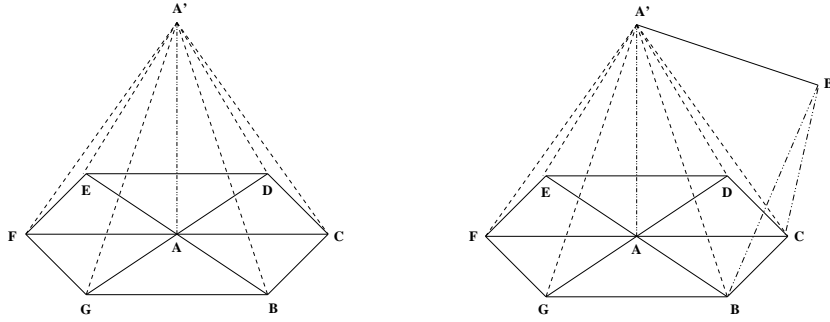


Figure 1. Left: A' is chosen to be the evolved counter-part of A . A and A' are connected via a time-like “vertical” edge. The rest of the vertices, i.e. B, C, \dots are connected to A' via space-like “diagonal” edges. Bones with two space-like and one time-like sides (SST) are formed in all triangles with one vertical and one diagonal edge. The length of 4 of the edges can be chosen arbitrarily.

Right: B' is the evolved counter-part of B . Again, BB' is a time-like edge but all other vertices, including A' are connected to B by space-like edges. $A'B'$ is the evolved counter-part of edge AB .

direction. In figure (1), suppose vertex A' is the evolved counter-part of vertex A (the un-primed vertices all reside on a spatial skeletonised foliation of a space-time). According to this algorithm, A and A' are to be connected by a “vertical” edge. In addition, all the vertices that were directly connected to A on the initial hypersurface, are to be connected to A' by “diagonal” edges. Thus, if A were directly connected to $n + 1$ struts that go between this hypersurface and the one to be built “above” it. The length of four of these newly added edges can be chosen arbitrarily, corresponding to the freedom in the choice of lapse and shift \ddagger . Solving the relevant Regge equations, one obtains the length of the rest of the struts. To build and later find the length of the edges in the next spatial hypersurface, one has to continue the above-mentioned procedure for each of the vertices of the initial hypersurface. The next step is very similar to this step, differing from it only in that the two new vertices, i.e. A' and B' , must also be connected. As shown in figure (1), $A'B'$ is the first edge of the next spatial hypersurface; the evolved counterpart of AB .

To our knowledge, PIES is by far the most efficient (3+1)-evolutionary method introduced in the context of Regge Calculus. The evolution of a space-like hypersurface can be achieved locally by evolving one vertex at a time and in parallel for those vertices which are not directly connected. Other evolutionary methods developed based on Regge Calculus use non-simplicial blocks. This is indeed a disadvantage as these methods require the introduction of information other than the edge lengths of the building blocks. PIES, however, has a big shortcoming: when Barrett et al. try to use this method to examine the evolution of a skeletonised spherical Friedmann-Lemaître-Robertson-Walker Universe, they find that the evolution stops well before

\ddagger The ADM formalism, developed by Arnowitt, Deser and Misner, foliates space-time into space-like hypersurfaces. The lapse function and shift vector indicate how these foliations are welded to each other. The freedom in choice of lapse and shift arises from the Bianchi identities. It is well known that Bianchi identities have a counterpart in Regge Calculus and this provides one with the advantage of choosing four of the edge lengths arbitrarily, similar to what is done in ADM formalism.

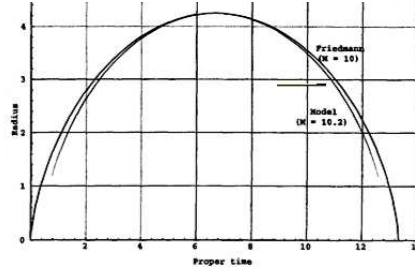


Figure 2. The Evolution of the spherical FLRW Universe using the 600-cell triangulation of 3-sphere as obtained by Barrett et al. The evolution stops well before reaching zero spatial volume [3].

the spatial volume of this universe even gets close to zero. A graph of the evolution of the skeletonised FLRW, as obtained by Barrett et al., is shown in figure (2). We believe that this problem has root in not accounting for causality correctly. In this paper, we show that by correctly accounting for causality the “stop point” problem will be resolved.

3. Area of a Bone and the Issue of Causality

In their seminal paper on PIES, Barrett et al. argue that since in this approach one tries to obtain the information about the newly introduced edges from the knowledge of the triangulation of the initial spatial hypersurface, the tent-like structure formed above a chosen vertex on a spatial hypersurface must reside within the future domain of dependence of this hypersurface. Thus, as shown in figure (3), the diagonal edges must be space-like while the vertical edge can in principle be time-like, null or space-like. The restriction as imposed by Barrett et al. is more a “No Collision” requirement than a causality requirement. What this condition does is that by making the diagonal edges space-like, prevent the time-like paths of evolving vertices from colliding in the future.

To include causality without violating the above-mentioned condition, one has to look at the past null cone of the evolved counterpart of a vertex. Figure (4) shows the situation in a (1+1)-dimensional space-time. It is quite clear that not the entire 1-d piece-wise linear space is within the past null cone of vertex A' . It is best to discuss causality in (3+1)-dimensional skeletonised space-times. Consider triangle $\triangle CAB$ in figure (5); suppose that CA is a space-like edge on a triangulated 3-dimensional spatial hypersurface. Following the PIES algorithm, assume vertex B is the evolved counterpart of vertex C . Edge BC is time-like but edges AB and CA are space-like as prescribed by the algorithm. CA resides on the initial hypersurface while BC and AB go between the two hypersurfaces. The null cone of vertex B divides the time-like bone $\triangle CAB$, into a triangle with two space-like and one null edge (NSS) and a triangle with one time-like, one space-like and one null edge (NST). Clearly, only the (NST) part of the bone is in the past domain of dependence of vertex B and could

§ A space-like bone is a bone made of only space-like edges. A time-like bone however is constructed from a combination of both time-like and space-like edges.

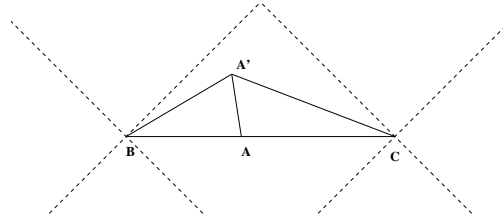


Figure 3. An illustration of PIES in a (1+1) skeletonised space-time. Barrett et al. require that the diagonal edges such as BA' be space-like while the evolutionary paths of vertices, such as AA' can be time-like, space-like or null. This condition only prevents the time-like evolutionary paths of vertices not to collide. This condition is a “No Collision” condition which results in a piece-wise linear congruence of non-intersecting paths of evolving vertices.

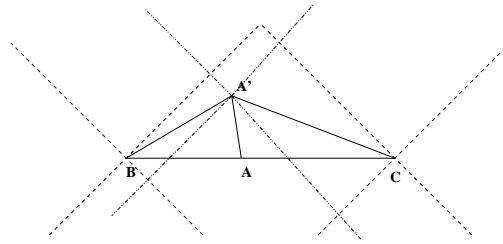


Figure 4. Only the information within the past null cone of A' could have affected it.

have had any influence on B . Thus to account for causality, we have to include this fact in the action.

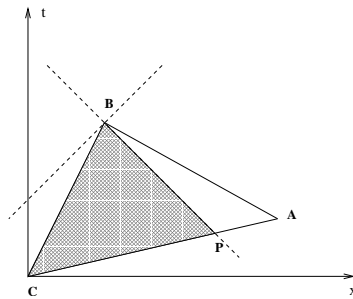


Figure 5. Vertex B is taken to be the evolved version of vertex C . Only the crossed-hatched area of triangle $\triangle CAB$ is within the null cone of vertex B .

It is well known that the action for a skeletonised space-time is given by [1]:

$$I = \sum_n A_n \epsilon_n \tag{1}$$

The Regge equation is obtained by varying this action with respect to a given edge. In his seminal paper, Regge showed that one can carry out this variation as if the

deficiencies were constant. The skeletonised version of Einstein's equation is then given by:

$$\sum_n \frac{\partial A_n}{\partial L_i} \epsilon_n = 0 \quad (2)$$

To include causality in the ‘‘Parallelisable Implicit Evolution Scheme’’, instead of the entire area of the bone in Regge action, only the part which is within the past null cone of vertex B must be included in the action. In particular, in writing the relevant Regge equations obtained by varying the area of a bone with respect to CB , one has to carry out this variation for the area of the (NST) triangle, $\triangle CBP$. We now carry out this variation for a time-like bone. A similar line of argument can be used to obtain similar results for a space-like bone.

4. Variation of a Time-Like Bone with respect to a Time-Like edge

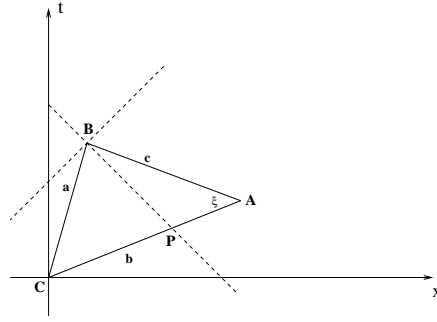


Figure 6. The time-like bone $\triangle CAB$ is divided into a NST and a NSS triangle by the null line passing through B .

Consider the time-like bone $\triangle CAB$ in figure (6). In this triangle we have:

$$A_{\triangle CBP} = A_{\triangle CAB} - A_{\triangle APB}$$

From (A.7), one has:

$$A_{\triangle CBP} = A_{\triangle CAB} - \frac{A_{\triangle CAB}}{2b^2}(a^2 + b^2 + c^2) + \frac{4A_{\triangle CAB}^2}{2b^2} \quad (3)$$

Varying the area of $\triangle CBP$ with respect to ‘‘ a ’’, the time-like edge of $\triangle CAB$, one has:

$$\frac{\partial A_{\triangle CBP}}{\partial a} = \frac{\partial A_{\triangle CAB}}{\partial a} \left(1 - \frac{a^2 + b^2 + c^2}{2b^2} + \frac{4A_{\triangle CAB}}{b^2}\right) - \frac{a}{b^2} A_{\triangle CAB} \quad (4)$$

but

$$\frac{\partial A_{\triangle CAB}}{\partial a} = \frac{1}{2} a \frac{(b^2 + a^2 + c^2)}{4A_{\triangle CAB}} = \frac{1}{2} a \coth \xi$$

Inserting this into equation (4) results in:

$$\frac{\partial A_{\triangle CBP}}{\partial a} = \frac{1}{2} a (\coth \xi) \left(1 - \frac{c}{b} \cosh \xi + \frac{2c}{b} \sinh \xi\right) - \frac{a}{b^2} A_{\triangle CAB}$$

where we have used

$$4A_{\Delta CAB}/b^2 = (2c/b) \sinh \xi \quad \text{and} \quad (c/b) \cosh \xi = (b^2 + a^2 + c^2)/2b^2.$$

One can simplify this equation by replacing $A_{\Delta CAB}$ with $\frac{1}{2}bc \sinh \xi$ to obtain:

$$\frac{\partial A_{\Delta CBP}}{\partial a} = \frac{1}{2}a \left(\coth \xi - \frac{c}{b} e^{-2\xi} \text{csch } \xi \right) \quad (5)$$

Finally, generalising equation (5) for all the bones hanging at edge a , one obtains the relevant Regge equation that must be used in a ‘‘causal PIES’’:

$$\sum_n \frac{1}{2}a \left[\coth \xi_n - \frac{c_n}{b_n} e^{-2\xi_n} \text{csch } \xi_n \right] \epsilon_n = 0 \quad (6)$$

where the sum is over all the bones meeting at the time-like edge ‘‘ a ’’ and ξ_n is the angle opposite to ‘‘ a ’’ in the n^{th} bone hanging at edge ‘‘ a ’’. ϵ_n stands for the deficiency associated with bone n .

5. Numerical Examples

In this section, we illustrate the revised algorithm by examining two skeletonised spherical FLRW universes. These numerical example are very close in nature to that given by Barret et al. and the details are quite similar. The interested reader is referred to section (6) of Barrett et al. paper [3]. The major difference between our solution and that of Barrett et al. is that, in obtaining these solutions, we have used our revised equation as obtained in the previous section. We have chosen the surfaces

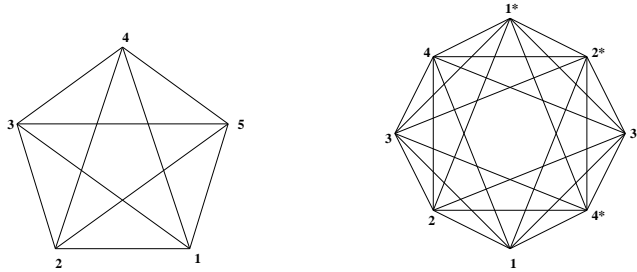


Figure 7. Pentatope (left) and Hexadecachoron (right) are standard triangulations of a 3-sphere.

of a pentatope (5-cell) as well as a hexadecachoron (16-cell), which are simple standard triangulations of a 3-sphere, shown in figure (7), as our underlying lattices. In addition, our choice of time function, as will be described below, is different from that of Barrett et al.

The evolution of the two models is very similar and thus we choose to discuss the pentatope universe. Assembling five dust particles on each of the vertices of a pentatope, we use the revised algorithm to evolve a given hypersurface in time. Each dust particle is taken to have a mass of $M/5$ where M is the total mass of the skeletonised universe. To compare the evolution of this skeletonised universe with the analytical solution, an ‘‘effective radius’’ is introduced. This effective radius or scale

factor of the lattice universe is obtained by equating the volume of the pentatope to the analytical volume of a 3-sphere at each step. More specifically, we have:

$$\frac{5l^3}{6\sqrt{2}} = 2\pi^2 a_e^3 \quad (7)$$

where l is the triangulation edge length and a_e is the so-called effective radius. We follow the contraction of this lattice universe from the moment of time symmetry on [5].

Another important issue in comparing the evolution of the skeletonised universe with the analytical solution is the choice of a correct time function. A straightforward analysis of the Robertson-Walker metric shows that the elapsed time between two consecutive skeletonised spatial hypersurfaces in continuum is given by the change in the 4-volume divided by the 3-volume of the initial hypersurface. Extending this analysis to the discretised regime, the lapse of time must be given by the 4-volume of the object sandwiched between two consecutive hypersurfaces, divided by the 3-volume of the base. However, the nature of the algorithm is such that this block has a very complicated construction and calculating the 4-volume is extremely hard. As a matter of fact, as will be discussed below, the notion of proper time is much more complicated in skeletonised space-times.

At first glance, the norm of the time-like edge [16] might appear to be a good candidate to represent the lapse of time. However this choice fails because of the very nature of the algorithm: as the curvature in a skeletonised space-time is concentrated on hinges, the space-time is flat everywhere else and thus all the line segments emanating from a vertex are portions of geodesics as shown in figure (8). The length of each of these line segments correspond to proper time intervals measured by different observers. These times are related to one another by Lorentz transformations. It is not however possible to distinguish which one of these observers is measuring the comoving time, since for each such observer, their proper time defines what they mean by cosmic time. Since there is not a unique comoving observer at each vertex, but a class of such observers, there is no unique comoving time, but a whole class of choices of comoving time. The notion of orthogonality at a vertex, in a piece-wise linear regime, is not well defined either. More specifically, the notion of an orthogonal vector at a cone singularity is not well defined. Thus it is not feasible to define a unique comoving time as is done in the continuous case using the Weyl postulate. Consequently, it is not possible to define a unique notion of comoving time for skeletonised space-times as in the continuum.

One solution to this problem is that instead of using the exact lapse of time, a measure of this lapse be obtained from the properties of the lattice that change with the evolution. We choose to represent the lapse of time with the volume of part of the 4-dimensional block, scaled by the edge length of the triangulation of the hypersurface that is being evolved. The volume of a 4-dimensional simplex, such as [12346], as illustrated in figure(9), is ideal. This particular choice of time, contains many properties of the initial hypersurface and its evolved counter-part ([1234] is a tetrahedral block in the initial hypersurface and [16] is an evolutionary step which is time-like). It is well known that the 4-volume is indeed a reasonable choice to represent the lapse of time [7]. We believe that our choice of time is appropriate as it embraces many evolutionary features of the algorithm. This choice however is proportional to

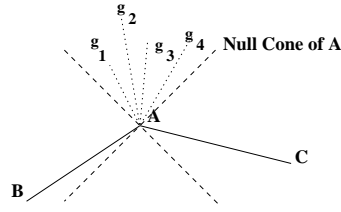


Figure 8. Any line segment emanating from vertex A and lying within the future null cone of A is a portion of a future-pointing time-like geodesic. The length of each of these is the proper time measured by the observer moving along that time-like line, but none can be preferred over the others.

the proper time and the constant of proportionality is a free parameter in our model.

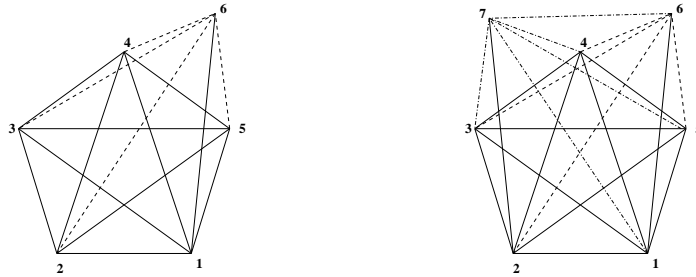


Figure 9. Evolving vertex [1] to [6] produces five 4-simplices, four of them contain the time-like edge [16] and are all equivalent. The one that does not contain edge [16] is purely space-like. The elapsed proper time is taken to be proportional to the 4-volume of one of the 4-simplices with a time-like edge.

To compare the revised algorithm with PIES, we make similar assumptions to Barrett et al. in that we take all the diagonal edges to be of equal length. In addition, we take the pentatopes, corresponding to the triangulation of a spatial 3-surfaces to be equilateral. Finally, all the vertical edges, connecting a vertex to its evolved counterpart, are taken to have equal lengths. These assumptions indeed correspond to a skeletonised isotropic and homogeneous universe. Following the algorithm and using the revised equations, one obtains two roots for the length of diagonal edges, one that corresponds to a contracting universe and one corresponding to a universe which expands indefinitely. Choosing the former and applying the algorithm one more time, say to vertex [2], we obtain two roots for the triangulation edge length of the next spatial hypersurface. The difference between the two roots, obtained in this step, is of the order of 10^{-2} and both lead into acceptable solutions.

The most important feature of this solution is that, independent of the choice of time function, the evolution does not stop at a finite spatial volume. This is indeed firm evidence for the fact that the introduction of causality in the algorithm resolves the problem of stop point. A curious feature of this solution is that the evolution becomes slower and slower as the spatial volume gets smaller and closer to zero. In particular, by taking the same evolutionary step, the change in the volume becomes

smaller as one gets closer to the zero spatial volume. Consequently, in principle, one might need take an infinite number of steps so that the spatial volume collapses to zero. We believe that one reason behind this behaviour is the “no collision” requirement as set by Barrett et al. Figure (10) shows the outcome of our numerical example for the 5-cell and 16-cell lattices. It is quite evident that although we have worked with much cruder underlying lattices, the evolution of our model is in good agreement with the analytical solution.

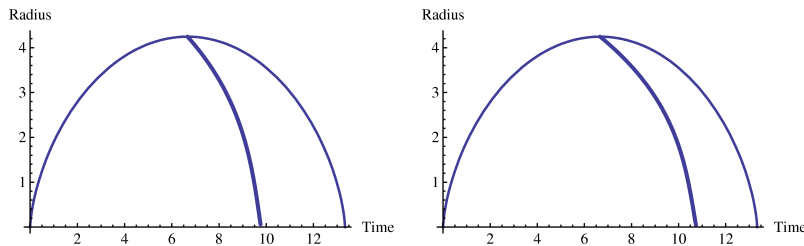


Figure 10. Left Panel: The Evolution of the Pentatope FLRW Universe. The mass of the analytical solution is taken to be $M = 10$. The mass of the skeletonised universe is 14.001 and the evolution steps are equal to 0.01. The constant of proportionality in the time-function is taken to be $1/20$. Right Panel: The Evolution of the Hexadecachoron FLRW Universe. The mass of the analytical solution is taken to be $M = 10$. The mass of the skeletonised universe is 12.052 and the evolution steps are equal to 0.01. The constant of proportionality in the time-function is taken to be $1/4$.

6. Conclusion

In this paper, we have shown how to account for causality in the “Parallelisable Implicit Evolutionary Scheme”. We obtained the relevant Regge equations that must be used in determining the unknown edge-lengths in this evolutionary method. The evolution of a skeletonised FLRW universe, using a 5-cell triangulation of a 3-sphere and a 16-cell triangulation, was examined. It was shown that the results of this approximation are in good agreement with the analytical model. The inclusion of causality in PIES is indeed an important step in making this evolutionary method into an excellent probe in investigating the evolution of complicated manifolds including those with non-trivial topology.

Appendix

Appendix A.1. Area of a SST Triangle

In Euclidean geometry, the area of any triangle can be obtained using Heron’s formula. For a triangle with edges a , b and c , Heron’s formula reads:

$$Area = \frac{1}{4} \sqrt{P(P-a)(P-b)(P-c)} \quad (\text{A.1})$$

where $2P$ is the perimeter of the triangle. This formula can be written in terms of the determinant of a matrix, known as the Cayley-Menger determinant:

$$Area^2 = -\frac{1}{16} \begin{vmatrix} 0 & 1 & 1 & 1 \\ 1 & 0 & b^2 & a^2 \\ 1 & b^2 & 0 & c^2 \\ 1 & a^2 & c^2 & 0 \end{vmatrix}.$$

It is possible to show that Heron's formula holds true for triangles on the Minkowski plane. The only catch is that instead of the length of the edges (a positive value) one has to put the norm of the edges, in particular account whether an edge is time-like, null or space-like. In addition, to account for the original classification of the bones by Regge [1], the negative sign, in front of the determinant must be eliminated. Using the Cayley-Menger determinant, the area of (SST) Triangle, $\triangle ABC$, shown in figure (6) is given by:

$$A_{\triangle CAB}^2 = \frac{1}{16} ((a^2 + c^2 + b^2)^2 - 4c^2b^2) \quad (A.2)$$

Appendix A.2. Area of a NSS Triangle

Another type of triangle whose area is required in obtaining equation (3) is a triangle with two space-like sides and one null side (NSS). $\triangle CAM$ in figure (A1) is a (NSS) triangle with sides \overline{CA} and \overline{AM} space-like and \overline{CM} null. The area of a (NSS) triangle can be obtained in a similar manner using a Cayley-Menger determinant:

$$A_{\triangle CAM}^2 = \frac{1}{16} (m + c)^2 (m - c)^2 \quad (A.3)$$

For the purpose of this work however, we require to write this area in a different form:

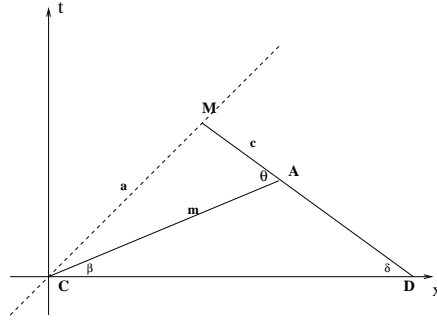


Figure A1. $\triangle CAM$ is a NSS Triangle with \overline{CM} being the null edge.

This expression of area will be given in terms of one of the space-like edges and the angle between the two space-like edges; start with

$$\overline{CA} + \overline{AM} = \overline{CM} \quad (A.4)$$

Taking the dot product of both sides of (A.4) with \overline{CM} and using the fact that \overline{CM} is null one obtains:

$$\overline{CA} \cdot \overline{CM} = -\overline{AM} \cdot \overline{CM}$$

Since \overline{CM} is a null vector in the first quadrant, it can always be written as:

$$\overline{CM} = a(\hat{t} + \hat{x})$$

where “ a ” is a real and positive number. Then:

$$\begin{aligned} a m (\cosh \beta - \sinh \beta) &= -a c (-\cosh \delta - \sinh \delta) \\ m (\cosh \beta - \sinh \beta) &= c (\cosh \delta + \sinh \delta) \end{aligned}$$

Solving for “ c ”, we have:

$$c = m \frac{(\cosh \beta - \sinh \beta)}{(\cosh \delta + \sinh \delta)}$$

which can be re-written as:

$$\begin{aligned} c &= m (\cosh \beta - \sinh \beta)(\cosh \delta - \sinh \delta) \\ &= m (\cosh (\delta + \beta) - \sinh (\delta + \beta)) \end{aligned}$$

In figure (A1), $\delta + \beta = \theta$ [6], and thus:

$$m = c (\cosh \theta + \sinh \theta)$$

Using this result in equation (A.3), one obtains:

$$A_{\Delta CAM} = \frac{1}{2} c^2 (\cosh \theta + \sinh \theta) \sinh \theta \quad (\text{A.5})$$

We will now use a similar strategy to obtain an expression for the area of ΔCBP as shown in figure (6). In this figure, the line segment BP is null and thus divides ΔCAB into an (NSS) and an (NST) triangle. To calculate the area of ΔCBP , it is easiest to subtract the area of ΔAPB from that of ΔCAB . Since ΔAPB is a (NSS) triangle, its area can be obtained using an equation similar to (A.5):

$$A_{\Delta ABP} = \frac{1}{2} c^2 (\cosh \xi - \sinh \xi) \sinh \xi$$

It is quite clear that $\sinh \xi = 2A_{\Delta CAB}/(bc)$ and $\cosh \xi = (b^2 + a^2 + c^2)/(bc)$; thus the area of ΔABP , in terms of the edge lengths, is given by:

$$A_{\Delta ABP} = \frac{A_{\Delta CAB}}{2b^2} ((a^2 + b^2 + c^2) - 4A_{\Delta CAB}) \quad (\text{A.6})$$

Since the area of ΔCBP is given by:

$$A_{\Delta CBP} = A_{\Delta CAB} - A_{\Delta APB}$$

one can use equation (A.6) to obtain the area of ΔCBP as

$$A_{\Delta CBP} = A_{\Delta CAB} - \frac{A_{\Delta CAB}}{2b^2} (a^2 + b^2 + c^2) + \frac{4A_{\Delta CAB}^2}{2b^2} \quad (\text{A.7})$$

The particular form of this equation facilitates the calculations of section (4).

References

- [1] Regge T 1961 *Nuovo Cimento* **19** 558.
- [2] Hamber H 2007 Discrete and Continuum Quantum Gravity, hep-ph/07042895.
- [3] Barrett J W, Galassi M, Miller W A, Sorkin R D, Tuckey P and Williams R M 1997 *Int. Journal of Theoretical Physics* **36** 4.
- [4] Sorkin R D 1975 *Phys. Rev. D* **12** 2.
- [5] Wheeler J A 1964 Geometrodynamics and the Issue of the Final State in *Relativity, Groups and Topology* (Gordon and Breach) p 316.
- [6] Birman G S and Nomizu K 1984 *The American Mathematical Monthly* **91** 9.
- [7] Sorkin R D 1994 *Int. Journal of Theoretical Physics* **33** 3.

